Supporting Information

Multicolor room-temperature phosphorescence induced by aggregation and TS-FRET of carbon dot composites

Jiayi Zhang[a], Wensheng Xu[a], Jiang Liu[a], Bin Li[a], Run Wang[a], Jianchao Ma[c], Linshuo Jiang[b], Yin Xiao[b], Yang Li[a,d], Xilong Yan[a,d], Ligong Chen[a,d], Bowei Wang[a,d]*

a. School of Chemical Engineering and Technology, Tianjin University Tianjin 300350 (P.R.China)

b. College of Chemistry and Chemical Engineering, Yulin University, Yulin 719000 (P.R.China)

c. College of Mining Engineering, Taiyuan University of Technology Taiyuan 030024 (P.R.China)

d. Tianjin Key Laboratory of Applied Catalysis Science and Technology,300350, (P. R. China)

E-mail: bwwang@tju.edu.cn (B.W.)

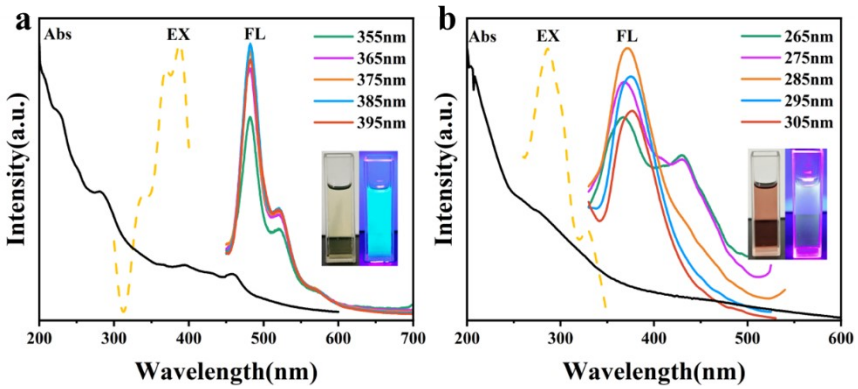

Fig.S1. UV-vis absorption, fluorescence excitation and emission spectra of a) PGCDs and b) CCCDs.

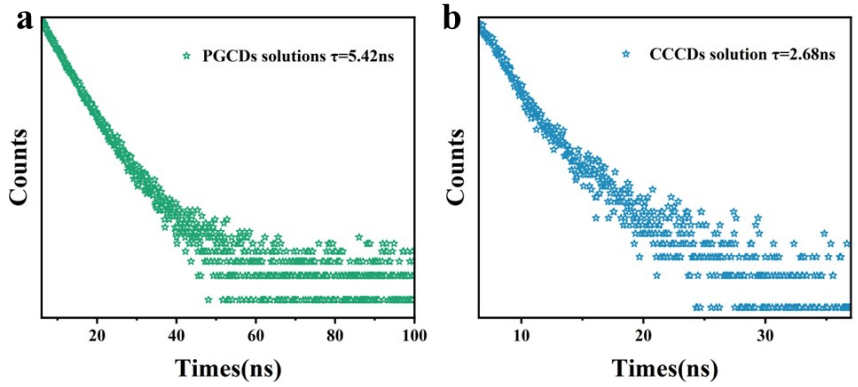

Fig.S2. FL decay curves of a) PGCDs and b) CCCDs in solution.

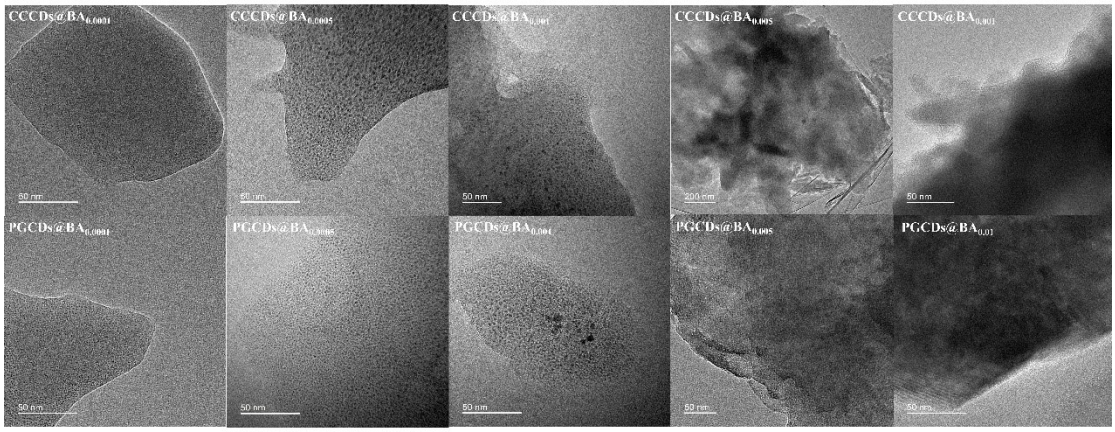

Fig.S3. TEM images of PGCDs@BA and CCCDs@BA powders with different doping concentrations.

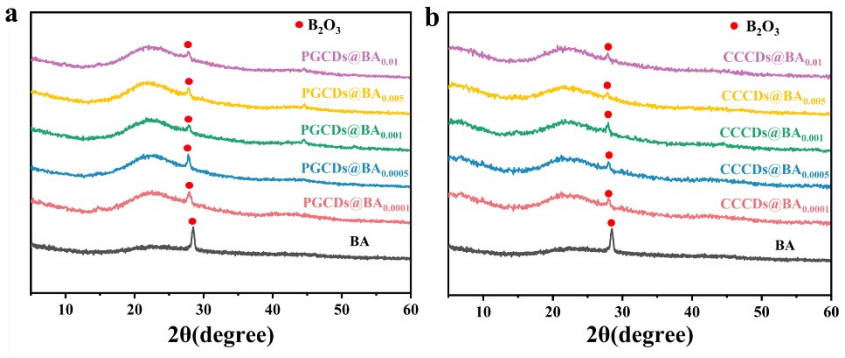

Fig.S4. XRD patterns of a) PGCD@BAx and b) CCCD@BAx.

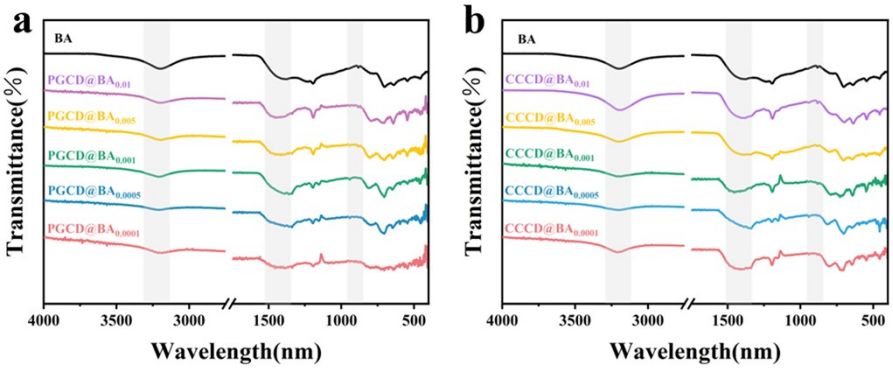

Fig.S5. FTIR spectra of a) PGCD@BAx and b) CCCD@BAx.

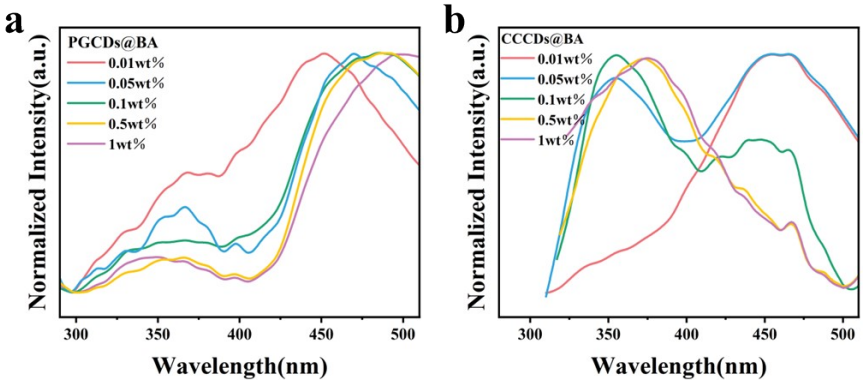

Fig.S6. Fluorescence spectra of a) PGCD@BAx and b) CCCD@BAx.

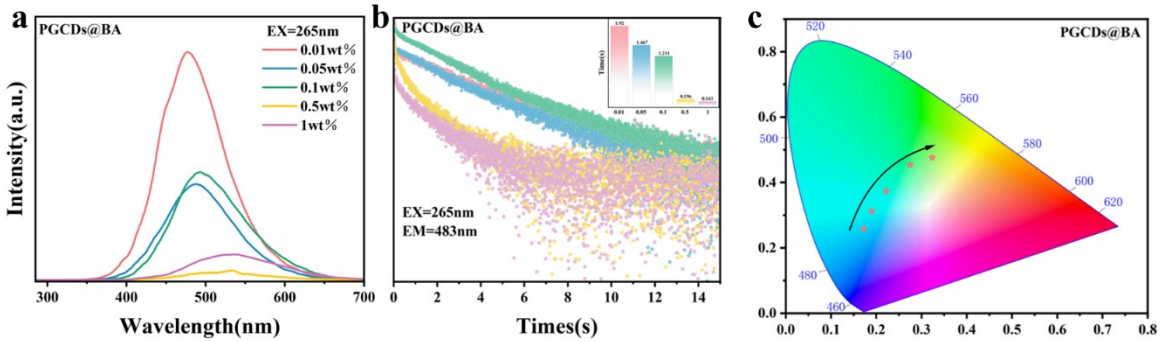

Fig. S7. a) Delayed PL spectra, b) lifetime decay profiles under 265 nm irradiation, and c) CIE coordinates of PGCDs@BA with different doping concentrations.

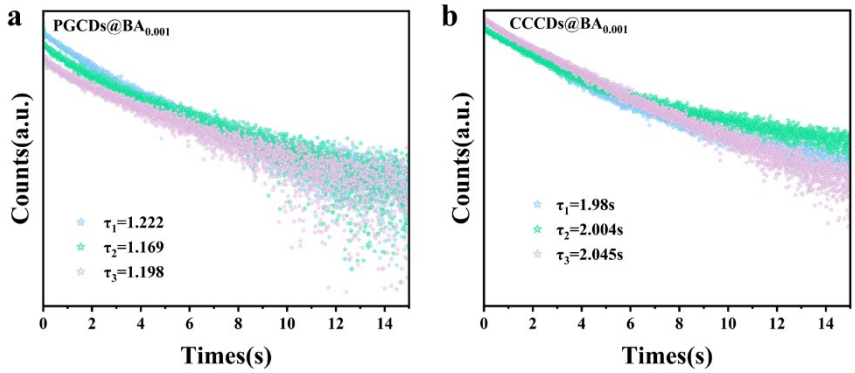

Figure.S8 Lifetime error bars for (a) CCCDs@$BA_{0.001}$ and (b)PGCDs@$BA_{0.001}$.

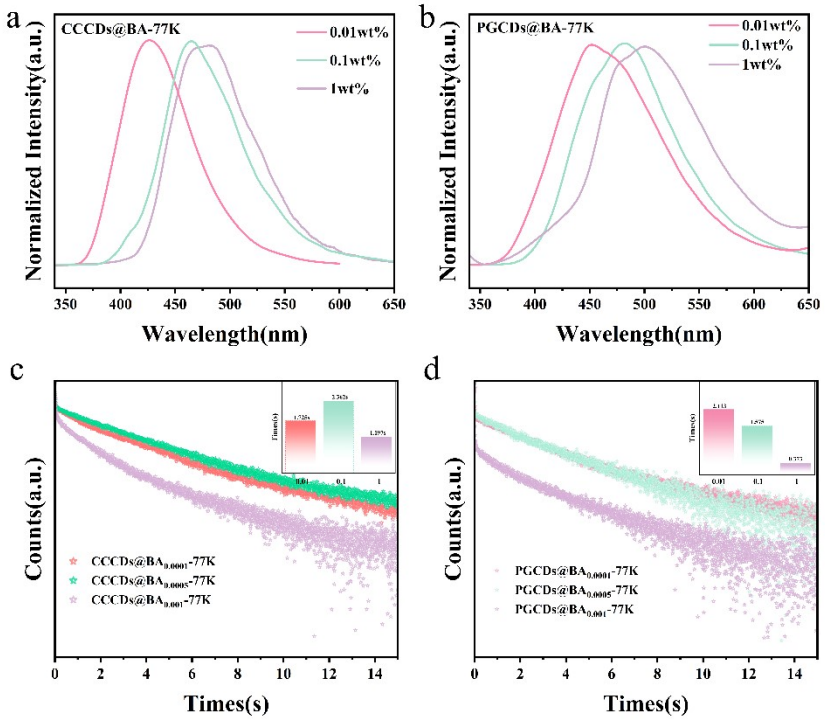

Fig.S9. 77 K phosphorescence spectra of (a) CCCDs and (b) PGCDs, and their corresponding lifetimes at 77 K (c and d), under different doping concentrations.

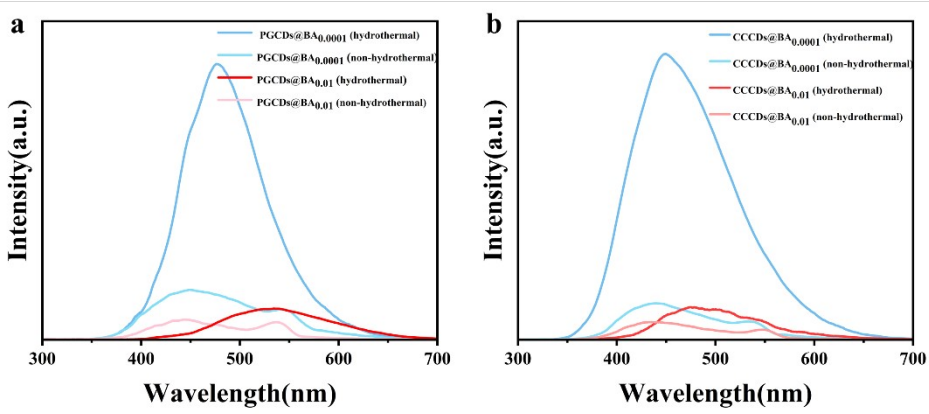

Fig. S10 (a) Comparison of spectra of PGCDs@$BA_{0.01}$ and PGCDs@$BA_{0.0001}$ before and after hydrothermal treatment; (b) Comparison of spectra of CCCDs@$BA_{0.01}$ and CCCDs@$BA_{0.0001}$ before and after hydrothermal treatment.

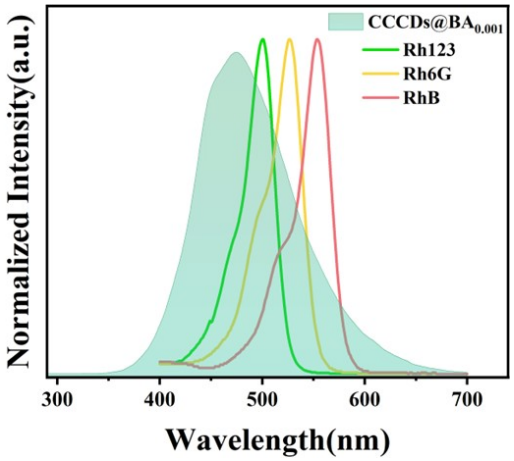

Fig.S11. Delayed PL spectrum (λex = 270 nm) of CCCDs@$BA_{0.001}$ and UV absorption spectra of fluorescent dyes (Rh123, Rh6G and RhB)

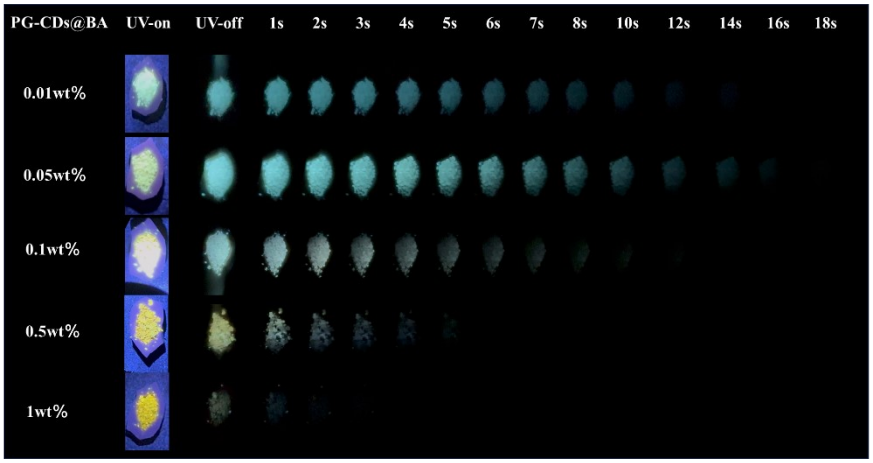

Fig.S12. Afterglow photos of PGCDs@BA powder with different doping concentration under 275 nm irradiation.

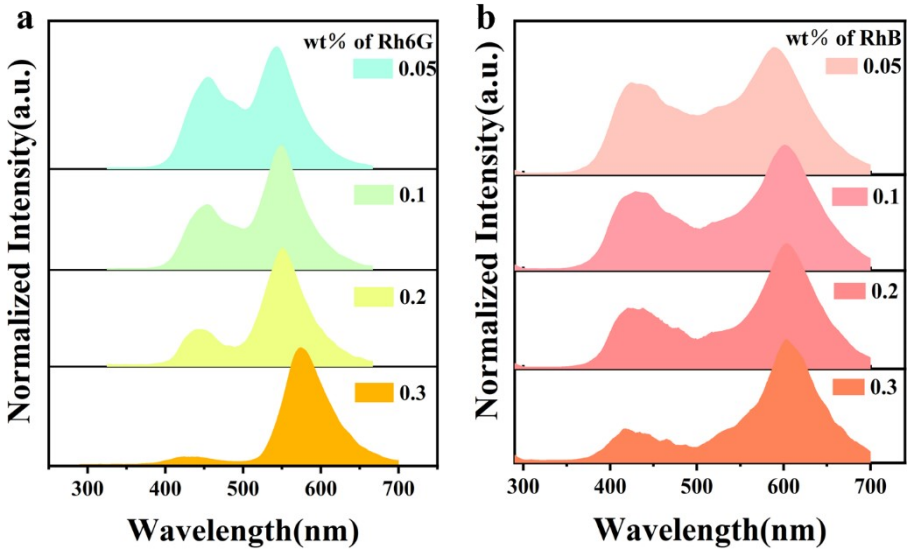

Fig.S13. Normalized delayed PL spectra of a) CCCDs@$BA_{0.001}$@Rh6G and b) CCCDs@$BA_{0.001}$@RhB.

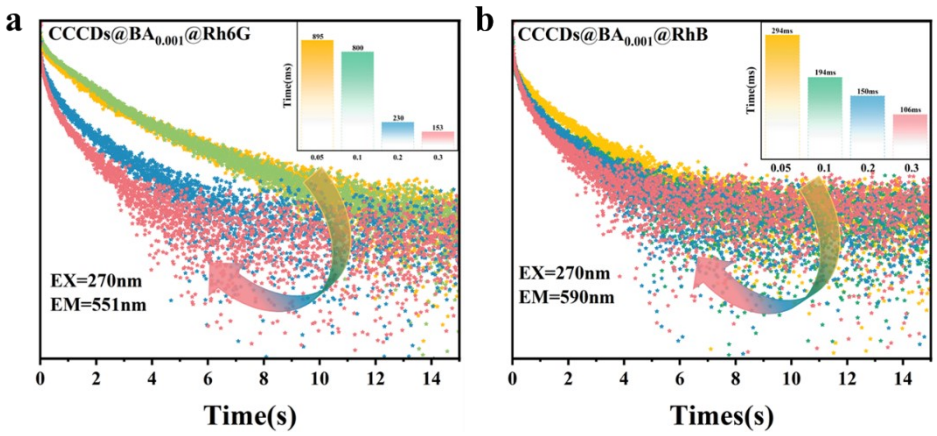

Fig.S14. Lifetime decay profiles of a) CCCDs@$BA_{0.001}$@Rh6G and b) CCCDs@$BA_{0.001}$@RhB powder with different doping concentration under 275 nm irradiation.

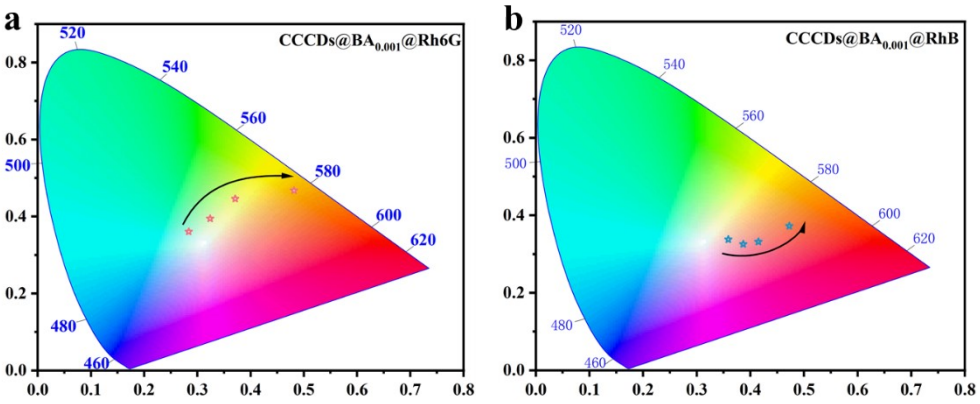

Fig.S15. CIE coordinates of afterglow emission of a) CCCDs@$BA_{0.001}$@Rh6G and b) CCCDs@$BA_{0.001}$@RhB powder.

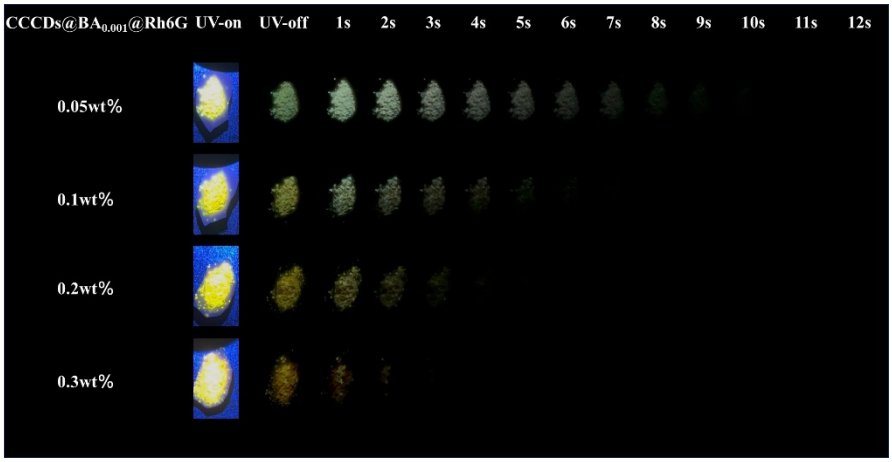

Fig.S16. Afterglow photos of CCCDs@$BA_{0.001}$@Rh6G powder with different doping concentration under 275 nm irradiation.

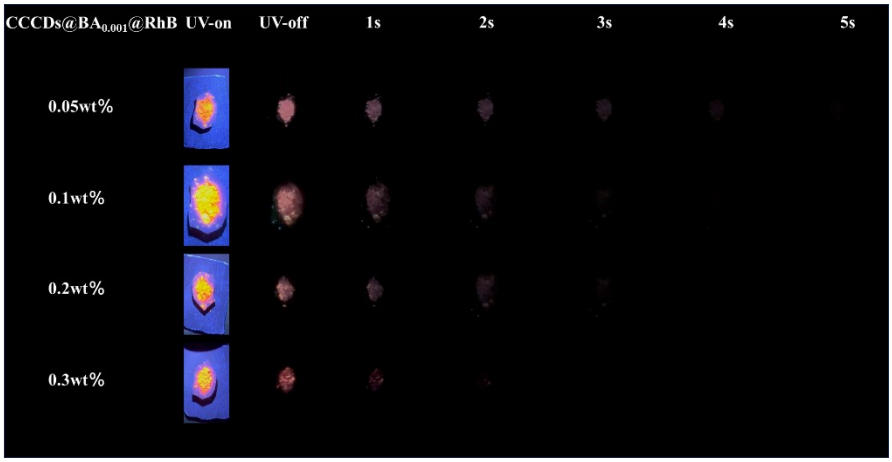

Fig.S17. Afterglow photos of CCCDs@$BA_{0.001}$@RhB powder with different doping concentration under 275 nm irradiation.

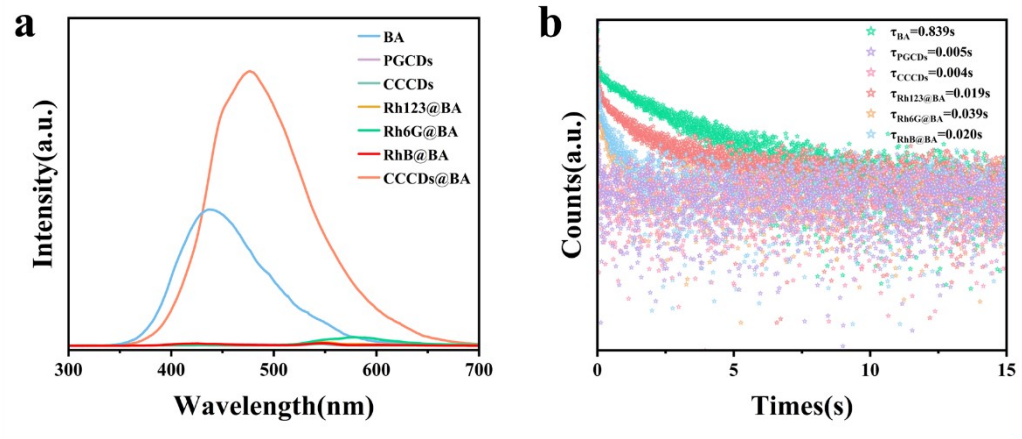

Fig.S18. Spectral comparison of pure BA,PGCDs,CCCDs, Rh123@BA, Rh6G@BA, RhB@BA, and CCCDs@$BA_{0.001}$ under identical hydrothermal conditions.

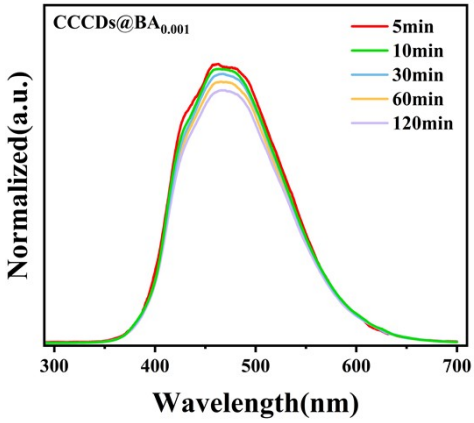

Fig.S19. Phosphorescence spectra of CCCDs@$BA_{0.001}$ under different irradiation times.

Table S1. Quantitative comparison between this work and recent related literature.

Work	Strategy	Emission tunability	Lifetime（s）	PL quantum yield (%)	Efficiency（%）
This work	CDs@BA Aggregation + TS-FRET	450-606	2.01	6.8	77.7
Li et al., CEJ 2023.[1]	Aggregation	530-750	1.66	32.8	N.R.
Teng et al., ACS ANM 2022.[2]	CDs@CNF TS-FRET	515-580	1.018	18	50
Lu et al., Spectrochim. Acta A 2024.[3]	CDs@SiO_2 FRET	503-570	1.10	1.36	N.R.
Jie et al., NJC 2023.[4]	CDs@BA	435-526	0.914	34.2	N.R.

Note: N.R. = not reported.

Table S2. Quantitative color analysis of PGCDs@BA composites.

Sample	CIE(x,y)	Δxy from previous	Color Purity (%)
PGCDs@$BA_{0.0001}$	(0.17,0.25)	0	55.2
PGCDs@$BA_{0.005}$	(0.19,0.31)	0.067	44.3
PGCDs@$BA_{0.001}$	(0.22,0.37)	0.137	37.9
PGCDs@$BA_{0.05}$	(0.27,0.45)	0.233	30.6
PGCDs@$BA_{0.01}$	(0.32,0.47)	0.286	29.1

Table S3. Quantitative color analysis of CCCDs@BA composites.

Sample	CIE(x,y)	Δxy from previous	Color Purity (%)
CCCDs@$BA_{0.0001}$	(0.17,0.20)	0	62.3
CCCDs@$BA_{0.005}$	(0.18,0.26)	0.063	48.7
CCCDs@$BA_{0.001}$	(0.19,0.27)	0.077	46.2
CCCDs@$BA_{0.05}$	(0.20,0.31)	0.118	39.5
CCCDs@$BA_{0.01}$	(0.20,0.32)	0.128	37.8

Table S4. Quantitative color analysis of CCCDs@BA@Rh123 composites.

Sample	CIE(x,y)	Δxy from previous	Color Purity (%)

CCCDs@$BA_{0.001}$@$Rh123_{0.05}$	(0.28,0.42)	0	36.1
CCCDs@$BA_{0.001}$@$Rh123_{0.1}$	(0.31,0.46)	0.050	34.0
CCCDs@$BA_{0.001}$@$Rh123_{0.2}$	(0.33,0.50)	0.095	33.8
CCCDs@$BA_{0.001}$@$Rh123_{0.3}$	(0.37,0.52)	0.140	32.0

Table S5. Quantitative color analysis of CCCDs@BA@Rh6G composites.

Sample	CIE(x,y)	Δxy from previous	Color Purity (%)
CCCDs@$BA_{0.001}$@$Rh6G_{0.05}$	(0.28,0.36)	0	38.9
CCCDs@$BA_{0.001}$@$Rh6G_{0.1}$	(0.32,0.39)	0.047	36.5
CCCDs@$BA_{0.001}$@$Rh6G_{0.2}$	(0.37,0.44)	0.114	34.8
CCCDs@$BA_{0.001}$@$Rh6G_{0.3}$	(0.48,0.46)	0.227	34.2

Table S6. Quantitative color analysis of CCCDs@BA@RhB composites.

Sample	CIE(x,y)	Δxy from previous	Color Purity (%)
CCCDs@$BA_{0.001}$@$RhB_{0.05}$	(0.35,0.33)	0	34.1
CCCDs@$BA_{0.001}$@$RhB_{0.1}$	(0.38,0.32)	0.031	32.5
CCCDs@$BA_{0.001}$@$RhB_{0.2}$	(0.41,0.33)	0.062	32.4
CCCDs@$BA_{0.001}$@$RhB_{0.3}$	(0.47,0.37)	0.134	33.0

Table S7 Summary of photophysical properties of PGCDs@BA powder at room temperature

Sample	λ_{em} (nm)	τ_p (s)	Φ_p (%)	k_p (s^{-1})	$k_{p,nr}$ (s^{-1})
PGCDs@$BA_{0.0001}$	478	1.92	5.92	0.0308	0.490
PGCDs@$BA_{0.0005}$	488	1.467	2.4	0.0164	0.665
PGCDs@$BA_{0.001}$	495	1.211	6.21	0.0513	0.775
PGCDs@$BA_{0.005}$	531	0.196	0.99	0.0505	5.05
PGCDs@$BA_{0.01}$	538	0.143	1.88	0.1315	6.86

λ_{em}: phosphorescence emission wavelength; τ_p: phosphorescence lifetime; Φ_p: phosphorescence quantum yield; k_p: radiative decay rate constant of phosphorescence; $k_{p,nr}$: non-radiative decay rate constant of phosphorescence.

Table S8 Summary of photophysical properties of CCCDs@BA powder at room temperature

Sample	λ_{em} (nm)	τ_p (s)	Φ_p (%)	k_p (s^{-1})	$k_{p,nr}$ (s^{-1})
CCCDs@$BA_{0.0001}$	450	1.334	5.3	0.0397	0.710
CCCDs@$BA_{0.0005}$	473	1.971	2.03	0.0103	0.497
CCCDs@$BA_{0.001}$	478	2.01	4.41	0.0219	0.476
CCCDs@$BA_{0.005}$	490	1.074	0.85	0.00792	0.923
CCCDs@$BA_{0.01}$	501	0.843	0.93	0.0110	1.175

λ_{em}: phosphorescence emission wavelength; τ_p: phosphorescence lifetime; Φ_p: phosphorescence quantum yield; k_p: radiative decay rate constant of phosphorescence; $k_{p,nr}$: non-radiative decay rate constant of phosphorescence.

Table S9. Energy transfer radius between the donor (CCCDs@BA0.001) and acceptors (Rh123, Rh6G and RhB).

Sample	$J(\lambda)$(T-S) ($nm^4\ M^{-1}\ cm^{-1}$)	R(T-S) (Å)
CCCDs@$BA_{0.001}$@Rh123	1.431×10^{15}	30.0
CCCDs@$BA_{0.001}$@Rh6G	2.152×10^{15}	32.4
CCCDs@$BA_{0.001}$@RhB	1.633×1015	30.7

$R^6 = 8.8 \times 10^{-5}$【$\kappa^2 n^{-4} \Phi_D J(\lambda)$】

Where κ^2 is the orientation factor of the molecular dipoles, n is the refractive index of the boric acid (BA) host, Φ_D is the quantum yield of the donor, and J(λ) is the spectral overlap integral between the donor emission and the acceptor absorption (calculated from the normalized emission spectrum of the donor and the molar absorptivity spectra of the acceptors Rh123, Rh6G, and RhB using the A|E 1.2 FluorTools software)

In this work, the orientation factor is taken as $\kappa^2=2/3$, assuming that the fluorophores are well separated and randomly oriented during the excitation process. The refractive index of the BA matrix is n=1.5, and the donor quantum yield is Φ_D=4.41%. Using the above formula and the spectral overlap integrals J(λ) the calculated Förster energy transfer radii R0 range from 21 to 33 Å. This range lies within the typical FRET-effective distance of 10–100 Å, thus fully satisfying the basic requirements for efficient energy transfer from the phosphorescent donor to the fluorescent acceptors.

Table S10 Energy transfer parameters between CCCDs@BA0.001 (donor) and different Dyes (acceptor)

Sample	wt% of Rh123	λ_{em} (nm)	τ_p (s)	Φp/f (%)	E (%)	k_{FRET} (s^{-1})
$CCCDs@BA_{0.001}$	-	476	2.01	4.41	-	-
$CCCDs@BA_{0.001}@Rh123$	0.05	476	1.146	9.36	43.0	0.376
		530	1.09			
	0.1	476	1.029	13.37	48.8	0.475
		530	0.645			
	0.2	476	0.634	7.74	68.5	1.081
		530	0.559			
	0.3	476	0.449	9.66	77.7	1.729
		530	0.202			
$CCCDs@BA_{0.001}@Rh6G$	0.05	476	1.389	4.89	30.9	0.222
		551	0.895			
	0.1	476	1.144	4.10	43.1	0.376
		551	0.8			
	0.2	476	0.797	5.12	60.4	0.757
		551	0.230			
	0.3	476	0.595	2.92	70.4	1.182
		551	0.153			
$CCCDs@BA_{0.001}@RhB$	0.05	476	1.218	3.08	39.4	0.323
		590	0.294			
	0.1	476	0.908	2.37	54.8	0.603
		590	0.194			
	0.2	476	0.798	2.18	60.3	0.755
		590	0.150			
	0.3	476	0.489	1.56	75.7	1.547
		590	0.106			

$E = 1 - \tau_{DA}/\tau_D$

$k_{FRET} = 1/\tau_{DA} - 1/\tau_D$

τ_{DA}: donor lifetime with acceptor; τ_D: donor lifetime without acceptor; E: energy transfer efficiency from donor to acceptor; k_{FRET}: FRET rate from the donor (478 nm) to the acceptor (530 nm).

Reference：

1 Q. Li, D. Cheng, H. Gu, D. Yang, Y. Li, S. Meng, Y. Zhao, Z. Tang, Y. Zhang, J. Tan and S. Qu, *Chemical Engineering Journal*, 2023, **462**, 142339.

2 X. Teng, X. Sun, W. Pan, Z. Song and J. Wang, *ACS Appl. Nano Mater.*, 2022, **5**, 5168–5175.

3 F. Lu, X. Xu, X. Zhu, L. Shen, W. Wan and M. Hu, *Spectrochimica Acta Part A: Molecular and Biomolecular Spectroscopy*, 2024, **304**, 123404.

4 Y. Jie, Y. Gao, D. Wang, F. Li, R. Chen, Y. Feng, W. Li and J. Fang, *New J. Chem.*, 2023, **47**, 16659–16665.